scientific reports

Check for updates

OPEN

Development of an objective index, neural activity score (NAS), reveals neural network ontogeny and treatment effects on microelectrode arrays

Austin P. Passaro[1,2], Onur Aydin[3], M. Taher A. Saif[3] & Steven L. Stice[1,2]✉

Microelectrode arrays (MEAs) are valuable tools for electrophysiological analysis, providing assessment of neural network health and development. Analysis can be complex, however, requiring intensive processing of large data sets consisting of many activity parameters, leading to information loss as studies subjectively report relatively few metrics in the interest of simplicity. In screening assays, many groups report simple overall activity (i.e. firing rate) but omit network connectivity changes (e.g. burst characteristics and synchrony) that may not be evident from basic parameters. Our goal was to develop an objective process to capture most of the valuable information gained from MEAs in neural development and toxicity studies. We implemented principal component analysis (PCA) to reduce the high dimensionality of MEA data. Upon analysis, we found the first principal component was strongly correlated to time, representing neural culture development; therefore, factor loadings were used to create a single index score—named neural activity score (NAS)—reflecting neural maturation. For validation, we applied NAS to studies analyzing various treatments. In all cases, NAS accurately recapitulated expected results, suggesting viability of NAS to measure network health and development. This approach may be adopted by other researchers using MEAs to analyze complicated treatment effects and multicellular interactions.

Micro- (or multi-)electrode arrays (MEAs) are valuable tools for network-level electrophysiological analysis of neuronal populations[1–4]. While sacrificing single cell resolution compared to traditional patch clamp electrophysiology, MEAs allow for recordings of entire neural networks both in vitro and in vivo and can be used to study dynamic network properties and development, either spontaneously or in response to stimulation or treatment. During recording, action potentials, or spikes, are detected via recording the corresponding voltage changes in the extracellular environment. Analysis of spike patterns provides network characteristics such as firing rate and network synchrony (see Supplementary Table S1 for list of all measured parameters), which are useful when determining neuronal network function and/or response to perturbation (i.e., stimulation or pharmacological treatment)[5,6].

Given these advantages, along with the advent of multi-well MEA plates that allow for higher-throughput screening and more complex experimental design, MEAs have seen widespread adoption from characterizing neural maturation to toxicity screening and drug development. Interestingly, despite the adoption of MEAs for these screening approaches, analysis has typically been limited to mean firing rate and other metrics of overall activity[7,8]. This limited analysis severely underutilizes MEA capabilities and may result in "false-negative" screening results, as only conditions or compounds that increase or decrease overall neural activity will be registered as hits with no regard to other aspects of neural network functionality or ontogeny. Current MEA analysis methods require the use of raster plots to visualize network development or individual parameter analysis, which are qualitative and difficult to interpret, respectively. While a general pattern of network development from sporadic spikes to sporadic bursts to coordinated synchronous network bursts has been well-described in previous studies[2,3,9,10], there is currently a lack of sufficient methods to quantify this observed ontogeny.

[1]Regenerative Bioscience Center, University of Georgia, Athens, GA, USA. [2]Division of Neuroscience, Biomedical Health and Sciences Institute, University of Georgia, Athens, GA, USA. [3]Department of Mechanical Science and Engineering, University of Illinois at Urbana-Champaign, Urbana, IL, USA. ✉email: sstice@uga.edu

Here, we developed a method implementing dimensionality reduction techniques, specifically principal component analysis (PCA), to create a singular index score—named neural activity score (NAS)—reflective of neural network ontogeny. NAS serves as an easily interpretable measurement to evaluate spontaneous network development in simple and complex cultures (i.e., neuron-glia co-cultures) or effects of various treatments (i.e., soluble factors or stimulation). We present validation of this method in several experiments, including a culture media comparison, various conditioned media treatments, and a microglia-neuron co-culture system, demonstrating the ability to measure both positive and negative effects on neural network activity and further interrogate toxicological screening, evaluating sensitivity on potential toxic compounds.

Results

Neural network ontogeny revealed by microelectrode array. Mouse embryonic stem cells were cultured and differentiated, resulting in cultures containing a mixture of motor neurons, excitatory and inhibitory neurons, and glial cells[11]. These neural cultures were allowed to mature on 48-well MEA plates over a 19-day period, typical for neuron maturation and network formation for these cells[12]. General spiking activity was detected at approximately 5 days post-seeding (days in vitro; DIV) and increased gradually throughout the recording period. Qualitatively, raster plots generated at various time points throughout the recording period demonstrate an expected pattern of network development: sparse and sporadic spikes appearing first, followed by sporadic bursts, followed eventually by synchronous network bursts (Fig. 1a–f). While this emergent development is evident from the raster plots, it is difficult to quantify. Quantification of several spike, burst, and network/synchrony metrics reveals general increases over time in these categories (Fig. 1g–n), but current MEA analysis methods do not allow for simple quantification of network ontogeny incorporating these and other activity metrics.

Principal component analysis of MEA parameters reveals temporal correlation, allowing for neural activity score derivation. Given the complexity and multivariate nature of the data, PCA was performed to reduce dimensionality and allow for easier visualization. After standard score normalization, all of the aforementioned parameters at all time points were included as data points for PCA. Examining the two-dimensional projection of the first two principal components revealed a distinct pattern in the data (Fig. 2a). Adding a dimension of time (via colormap), this pattern was revealed to be a temporal separation of the data points, especially along the first principal component. Statistically, linear regression analysis supported this temporal component, as principal component 1 (PC1) is strongly correlated to time (Fig. 2b; $R^2 = 0.5441$, $p < 0.0001$), indicating recapitulation of network ontogeny and maturation. After confirmation of this relationship, factor loading values for PC1 were examined to determine which factors (MEA parameters) contributed most strongly to this component. While substantial contributions were observed for many parameters, the strongest metrics were burst percentage, network burst percentage, number of spikes per burst, number of bursting electrodes, number of spikes per network burst, and synchrony index (Table 1). Notably, mean firing rate, the most common parameter analyzed in MEA studies, was the 11th-strongest contributor. Finally, these factor loading values were used to develop an individual index score—NAS (Eq. 1; see "Methods"). As NAS represents all aspects of neural network activity, it allows for assessment of neuronal network ontogeny and evaluation of the effects of various perturbations, such as stimulation, pharmacological treatment, or alternative culture conditions, which can typically be difficult to analyze if various parameters do not exhibit unidirectional changes. Additionally, NAS reduces the high variation often observed in individual MEA parameters, as evidenced by lower coefficient of variation for 24/25 (96%) measured parameters (Supplementary Fig. S1).

Enhancement of neural network ontogeny is easily quantified via NAS. Regression analysis served as initial support that NAS accurately measures neural network ontogeny, but we also sought to experimentally validate NAS in several conditions to further confirm this recapitulation. For initial validation, several experiments were performed to analyze enhanced neural network ontogeny and activity in response to different conditions known to enhance neural activity—namely, optimized culture media[13] and muscle-conditioned media treatment[14]. To examine the effects of optimized culture media, mixed neural cultures (HBG3-derived) were grown on MEAs in two different media conditions: DMEM/F12 & Neurobasal-based medium (DMNB) or BrainPhys-based medium (BP). While DMNB has traditionally been widely used to culture HBG3-derived and other neural cell lines, BP was developed for electrophysiological applications due to a more physiologically relevant formulation, resulting in increased electrophysiological function of various cell lines[13]. However, BP has not been evaluated on HBG3-derived neural cultures. In both DMNB and BP groups, the neurons began showing activity at approximately day 5, increasing over 3 weeks, as expected; however, the cells cultured in BP exhibited enhanced activity and network development, as indicated by the significantly higher NAS (Fig. 3a; $p < 0.0001$, two-way repeated measures ANOVA).

To examine the effects of conditioned media on network ontogeny, mixed neural cells were treated with muscle cell (C2C12)-conditioned media (CM), which has previously been shown to significantly accelerate network activity and development[14]. Likewise, NAS analysis showed similar results and provided simple quantification (Fig. 3b; $p < 0.0001$, two-way repeated measures ANOVA) of this accelerated network development.

Disruption of neural network ontogeny is easily quantified via NAS. In addition to measuring neural network activity enhancement, we also sought to validate NAS on more complex culture conditions and for quantifying disruption of network activity. Microglia, the resident immune cells of the central nervous system (CNS), are being increasingly implicated in neurodegenerative diseases and have been shown to be neurotoxic in many conditions[15–18]; therefore, we decided to explore co-culturing microglia with mixed neural cultures on

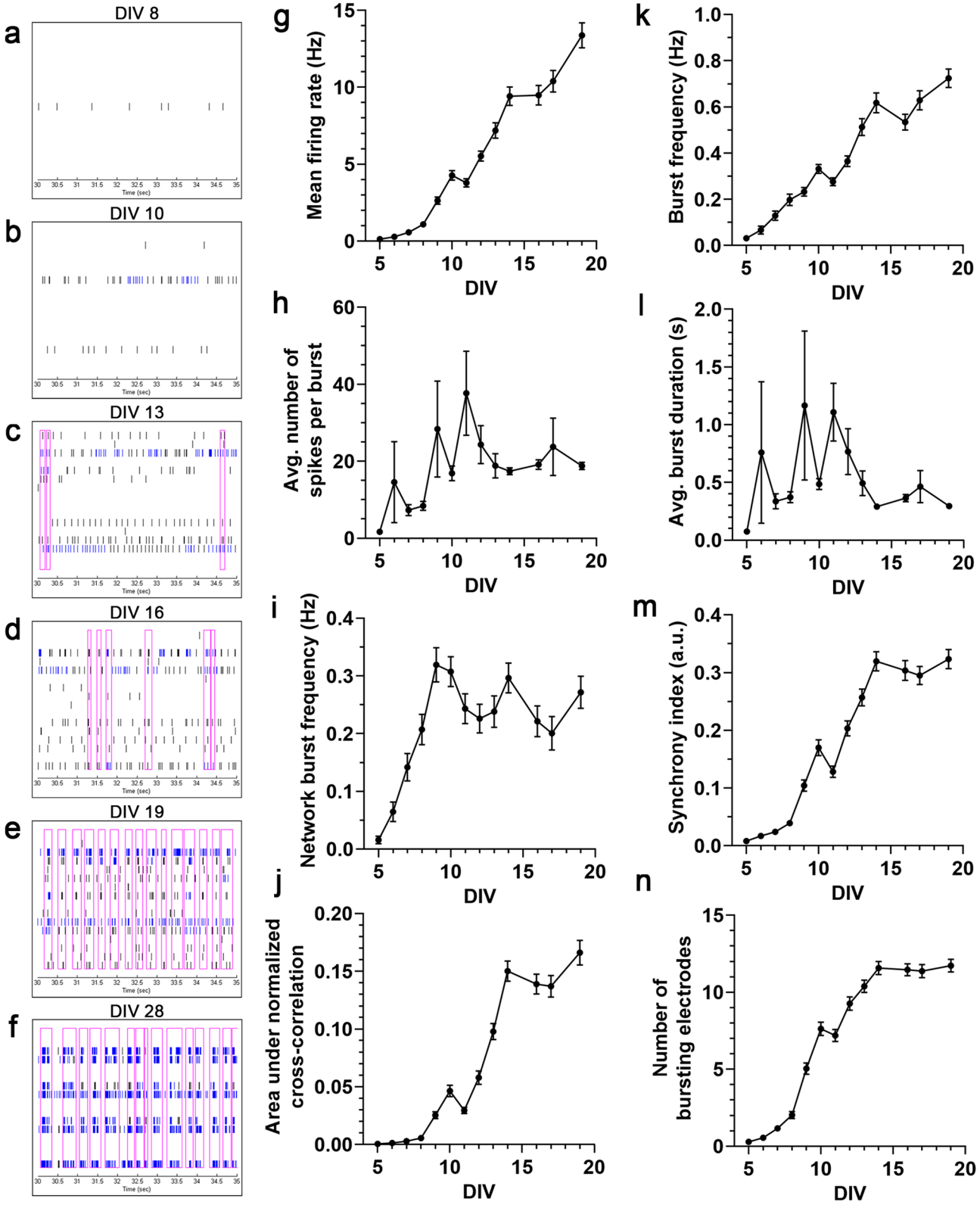

Figure 1. Neural network ontogeny revealed by microelectrode array. (**a**–**f**) Representative raster plots of one well over time, demonstrating qualitative network development. Each plot is 5 s for sufficient spike and burst resolution, and horizontal rows correspond to one channel/electrode, each. Note the changes over time: few spikes on few channels (DIV 8) to more spikes on more channels (DIV 10) to sporadic bursts (DIV 13, 16) to rhythmic network bursts (DIV 19) to stronger, rhythmic network bursts (DIV 28). (**g**–**n**) Line graphs of 8 example individual MEA parameters covering major categories (activity, bursting, network bursting, synchrony). Raster plots generated with Neural Metric Tool v1.2.3 software (Axion Biosystems): https://www.axionbiosystems.com/products/software/neural-module#applications.

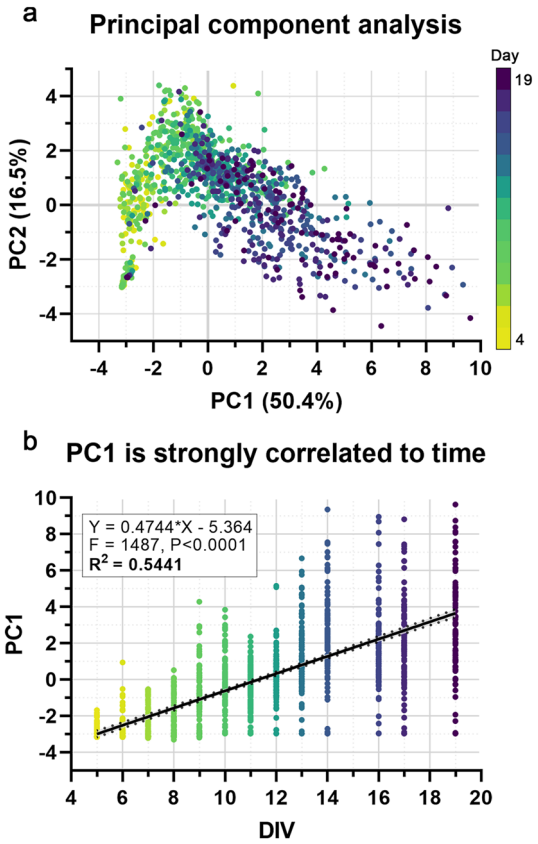

Figure 2. Principal component analysis of MEA parameters reveals temporal correlation. (**a**) The first two principal components (accounting for 66.9% of total variation), colored by time (yellow > green > blue > purple), showing a distinct pattern of separation/progression. (**b**) Principal component 1 (PC1) is positively correlated with time. Linear regression analysis confirms this strong correlation ($R^2 = 0.5541$, $F = 1487$, $p < 0.0001$).

MEAs. After allowing neurons to become active over 10 days, BV2 cells, an immortalized mouse microglia cell line, were added to the cultures at 8 different cell densities. We observed rapid disruption in network function in a clear cell density-dependent manner, with higher numbers of microglia relative to the neuronal population resulting in accelerated network disruption, as indicated by a decrease in NAS (Fig. 4a; $p < 0.0001$, two-way repeated measures ANOVA, Tukey's post-hoc test).

To examine whether this disruption is contact-dependent or the result of secreted factors, neural cultures were treated with BV2-conditioned media at 10 days (similarly to the co-culture experiment described above). Similar to the co-culture condition, BV2-conditioned media treatment also disrupted network function (Fig. 4b), suggesting a role for microglia-secreted factors in neural network disruption. To examine whether this effect was exacerbated by microglial activation, BV2 cells were stimulated with two concentrations of the pro-inflammatory endotoxin lipopolysaccharide (LPS; 10 ng/mL and 100 ng/mL) for 24 h prior to conditioned media collection. LPS-stimulated BV2-conditioned media disrupted network function in a concentration-dependent manner, with unstimulated BV2-conditioned media causing significant disruption ($p < 0.0193$, two-way mixed model, Tukey's post-hoc test), followed by 10 ng/mL LPS stimulation ($p = 0.0003$) and 100 ng/mL LPS stimulation ($p < 0.0001$), providing further support for NAS as a viable method to quantify complex treatment effects and evaluate disruption of electrophysiological function.

NAS summarizes neural activity for neurotoxicology screening. Advances in MEA technology[8,19] have led to adoption of MEAs for neurotoxicological screening[20] Given the potential of NAS to consolidate many functional MEA parameters, we sought to determine its applicability to neurotoxicity screening.

For this analysis, NAS values were calculated from MEA toxicity screening of 52 compounds from the NTP or ToxCast libraries[21,22] (Fig. 5a–c). In previous studies[21,22], the authors performed a network formation assay (NFA) using primary cortical neurons, measuring 17 parameters of activity in response to compound treatment over 12 days on MEAs to determine compound effects on network formation. Additionally, viability testing was performed to measure cytotoxicity. For each of these assays, EC_{50} values were determined for each compound. Here, we used NAS values to calculate and compare EC_{50} values to individual MEA parameter EC_{50} values and cytotoxicity EC_{50} values (Fig. 5d–f, Supplementary Table S2).

Of the 52 compounds we analyzed, 33 were found to have measurable effects in the network formation assay (defined as a decrease in activity by 3× median absolute deviation from control) for at least one activity parameter (though the specific parameter(s) differed among compounds), and 26 compounds were found to

Parameter	PC1	PC2	PC3	PC4	PC5
Burst percentage—Avg	0.938953	− 0.21655	− 0.09068	0.095365	− 0.03905
Network burst percentage	0.930335	− 0.16411	− 0.03479	− 0.00912	0.030603
Number of spikes per burst—Avg	0.927633	− 0.07813	0.131878	0.180872	− 0.20604
Number of bursting electrodes	0.924737	0.11382	− 0.13932	− 0.05683	− 0.03851
Number of spikes per network burst per channel—Avg	0.916818	− 0.09696	0.059892	− 0.0695	− 0.30286
Synchrony index	0.91299	− 0.25337	− 0.09404	0.126219	− 0.03106
Number of spikes per network burst—Avg	0.90668	− 0.14074	0.063698	− 0.03136	− 0.3157
ISI coefficient of variation—Avg	0.875459	− 0.13787	− 0.14411	0.203831	− 0.09526
Area under normalized cross-correlation	0.866748	− 0.32439	− 0.0838	0.14749	− 0.01187
Number of elecs participating in burst—Avg	0.866593	0.127533	− 0.16016	− 0.10207	− 0.04436
Mean firing rate (Hz)	0.787233	− 0.09261	0.483835	− 0.01736	0.111684
Network IBI coefficient of variation	0.739427	0.22799	− 0.36458	− 0.23674	0.12618
Burst duration—Avg (s)	0.730618	0.521412	0.032794	0.197191	− 0.12086
Normalized duration IQR—Avg	0.707402	0.327012	− 0.30471	0.026697	0.337296
IBI coefficient of variation—Avg	0.64845	0.459111	− 0.30775	0.114136	0.20907
Network normalized duration IQR	0.613893	0.064961	− 0.38534	− 0.17934	0.144007
Area under cross-correlation	0.606648	− 0.40216	0.517657	0.237669	− 0.14355
Burst frequency—Avg (Hz)	0.592944	− 0.04631	0.437397	0.034638	0.423479
Network burst frequency (Hz)	0.506543	− 0.0198	0.364146	− 0.01999	0.590348
Network burst duration—Avg (s)	0.490791	0.412156	0.078862	− 0.54881	− 0.07344
Width at half height of cross-correlation	0.233083	0.626106	0.385101	− 0.42764	− 0.13819
Width at half height of normalized cross-correlation	0.175127	0.727927	0.205821	− 0.28793	− 0.18294
Mean ISI within burst—Avg	0.029257	0.891807	0.112554	0.360375	0.016162
Median ISI within burst—Avg	− 0.05205	0.881542	0.1378	0.359244	0.017994
Inter-burst interval—Avg (s)	− 0.27591	0.571143	− 0.11858	0.370944	− 0.15048

Table 1. Factor loading values for principal components 1–5 for all MEA parameters analyzed. Parameters sorted by descending PC1 loading value.

have measurable cytotoxicity in the viability assay[21] (Fig. 5g). Similarly, using NAS EC_{50} values, we found 26/52 compounds (50%) affected neural activity (Fig. 5g). For these compounds, we compared the EC_{50} calculated from NAS to determine sensitivity compared to the average individual MEA parameter EC_{50} values and cytotoxicity EC_{50} values. We found NAS to be more sensitive (lower EC_{50}) than the average of all parameters for 16/26 compounds (61.5%) and more sensitive than the average cytotoxicity EC_{50} for 18/26 compounds (69.2%) (Fig. 5g, Supplementary Table S2).

Discussion

Advances in MEA technology, including multi-well MEA plates, incubated recording setups, and constantly improving software, allow for higher throughput than previously possible[18,19], though analysis has traditionally been limited to simple parameters, primarily mean firing rate. Only recently have researchers begun incorporating advanced metrics of network activity in these screening approaches[20–22]. These advanced metrics have provided researchers with tools to record from entire neuronal populations and analyze complex neuronal network dynamics. Multi-well MEAs enable high-throughput neuronal recordings, facilitating their adoption for drug/toxicity screening applications and evaluation of complex culture conditions. However, the information that can be gleaned from MEAs has been hampered by limited analytical methods and tools, as well as high variation. Here, we present a novel method to overcome these limitations—development of an index, neural activity score, that incorporates and consolidates traditional MEA measurements into a single quantitative value that can be used to objectively evaluate neuronal network development and function across various culture conditions, treatments, and neural cell sources. This is valuable not only for basic neuroscience research on neuronal networks, but also translational research and preclinical studies. To facilitate adoption, further validation, and improvement, codes used to calculate NAS can be found at the following open source repository: https://doi.org/10.5281/zenodo.3939310.

Despite these advantages, NAS is not free from its own limitations—particularly those associated with its derivation from principal component analysis. As NAS is essentially a linear weighted combination of individual activity parameters, parameters changing in equal (weighted) magnitude but in opposite directions could negate each other, resulting in no net change. While this example demonstrates the potential for different electrophysiological profiles with identical NAS, the overall goal of NAS is to provide a holistic interpretation of neural development and maturity, suggesting that these "equal but opposite" changes still represent cultures with similar overall states of maturation. For example, a culture with increased firing rate but decreased synchrony may represent an overall similar level of maturity—especially when comparing different cell types or culture conditions that may exhibit variations in ontogeny. NAS provides a way to "balance" these changes that would be difficult

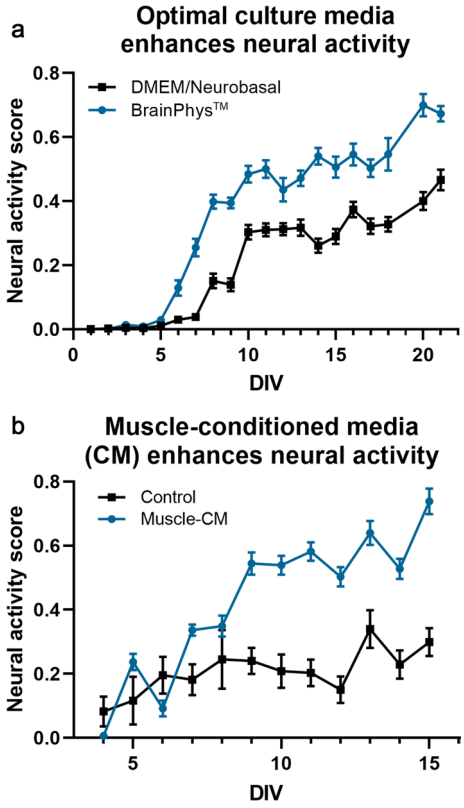

Figure 3. Enhancement of neural network ontogeny is easily quantified using neural activity score. (**a**) BrainPhys-based culture media results in clear enhancement of neural activity compared to traditional DMEM/Neurobasal-based media, and this enhancement is quantifiable via NAS ($p < 0.0001$, two-way repeated measures ANOVA, n = 24/group). (**b**) Muscle-conditioned media treatment results in similar enhancement of neural activity ($p < 0.0001$, two-way repeated measures ANOVA, n = 12/group).

to compare and interpret individually; however, these are important considerations to take into account during interpretation depending on the question of interest.

Another potential limitation is sensitivity to detect meaningful changes compared to noise, which is difficult to evaluate. Technologically, this sensitivity is determined by the MEA platform, recording settings, and analysis thresholds, such as the thresholds for determining spikes and bursts. For NAS, this sensitivity relies on the particular changes in activity. In one case, minute changes in multiple parameters in the same direction are summed, which would be measured as a larger overall change in NAS than the individual changes; however, in cases such as the one described above, small changes in opposite directions may go undetected. While this case may result in relatively low sensitivity, it also reduces variation, providing additional confidence that detected changes represent meaningful development and maturation.

One final limitation involves incorporation into existing analytical pipelines. While we encourage use and modification of the provided code and formulas to calculate NAS, we recognize that these are additional elements and steps to add to already complex pipelines and software packages that vary across individual labs and equipment. These extra steps may hinder rapid adoption for users with different MEA platforms and custom analyses, especially in other programming languages (e.g., MATLAB, R).

The results presented here demonstrate the value of NAS to assess potential developmental neurotoxicity (DNT) hazards, a field with a widely recognized need for more sensitive, less variable, and higher throughput functional assays[21–24]. The mixed neural cultures used for NAS derivation and the primary cultures analyzed in the network formation assay are both maturing networks, derived from embryonic stem cells or isolated from neonatal rodents, respectively. As a result, NAS is well-suited for analysis of maturing neural networks, as is necessary in DNT studies, covering a range from non-active to full maturity, with synchronized network bursting. The application to developing networks from multiple cell sources suggest NAS has substantial value for improving the use of MEAs for toxicity screening and drug development.

As the concern over drug development costs continues to rise, scientists are noticing several recurring problems, including the reproducibility crisis and inadequacies of current screening assays, in vivo models, and other preclinical studies[25–27]. For neural assays, specifically, assays have traditionally used simple endpoints such as viability and morphological analysis (i.e. neurite outgrowth) for screening, primarily due to scalability[28]. However, electrophysiological endpoints are often more sensitive and allow for assessment of electrophysiological toxicity, which involves separate—and highly time-sensitive—mechanisms[8,29,30]. By improving result

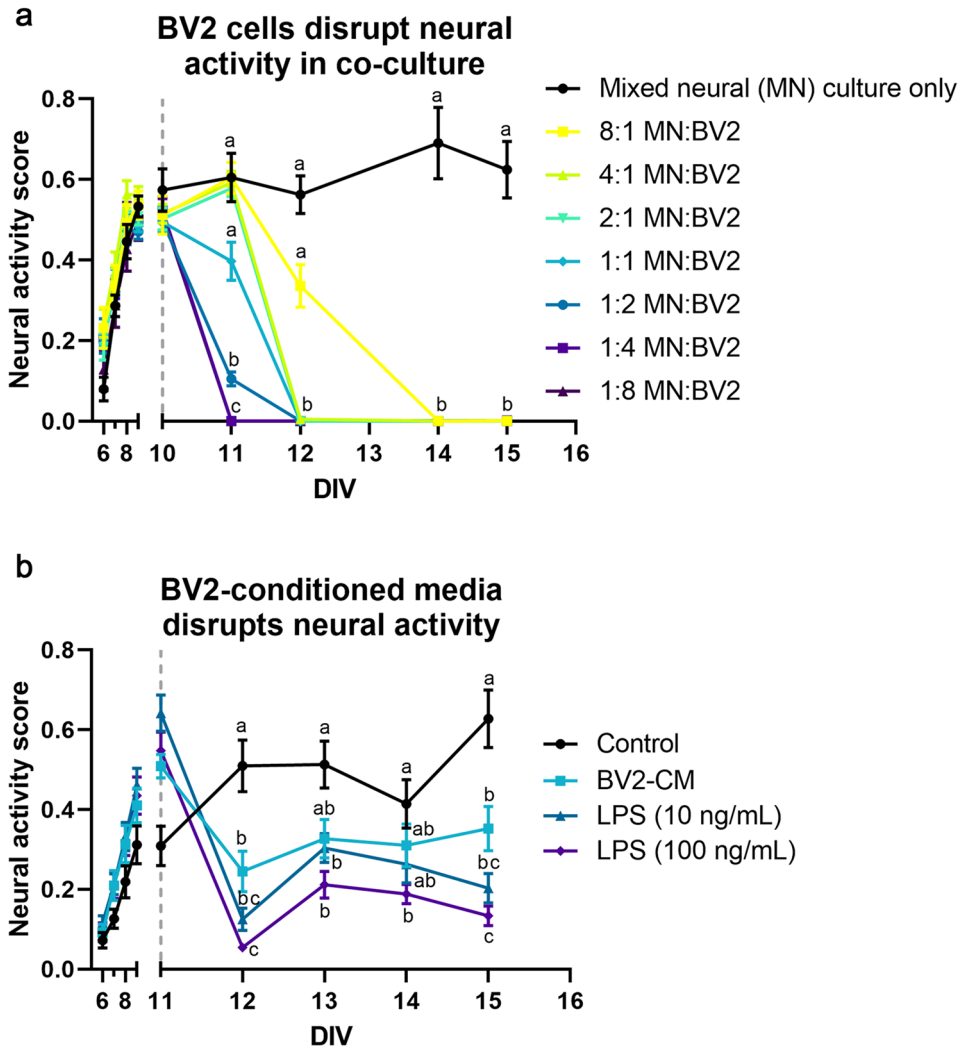

Figure 4. Disruption of neural network ontogeny is easily quantified using neural activity score. (**a**) Co-culturing mixed neural cultures and microglia (BV2 cells) results in a microglia concentration-dependent disruption of neural activity ($p < 0.0001$, two-way repeated measures ANOVA, Tukey's post-hoc test, $n = 6$/group). (**b**) Similarly, BV2-conditioned media treatment resulted in a similar decrease ($p < 0.0193$, two-way mixed ANOVA, Tukey's post-hoc test). Additionally, 24-h LPS treatment of BV2s prior to conditioned media collection exacerbated this disruption in a concentration-dependent manner (10 ng/mL, $p = 0.0003$; 100 ng/mL, $p < 0.0001$) ($n = 14$/group except media control group, for which $n = 12$). Grey dashed lines indicate time of BV2 or CM addition. Reported statistics are Tukey's post-hoc comparisons 24 h post-addition. Connecting letters on graphs indicate comparisons for other time points.

interpretation, NAS will facilitate incorporation of functional measures into screening programs focused on cytotoxicity and morphology.

Index scoring has been used extensively in clinical settings and in vivo; for example, neurological deficits in amyotrophic lateral sclerosis (ALS) and Parkinson's disease (PD) are assessed using the Revised ALS Functional Rating Scale (ALSFRS-R)[31] and United Parkinson's Disease Rating Scale (UPDRS)[32], respectively. Stroke severity is frequently measured using various scales [i.e., modified Rankin scale (mRS)[33,34] and NIH stroke scale (NIHSS)][35], and these have been shown to correlate strongly with patient outcomes and be useful for therapeutic evaluation[34]. The simplified analytical pipeline provided by these indices is vital to detecting effects (or lack thereof) in clinical and preclinical studies. Due to this, a need has been recognized to develop multivariate approaches and index scores for in vitro approaches, as well[36,37]. Similar analysis pipelines provided by index scores could be especially valuable for screening assays, allowing for improved hit detection when screening potential neurotoxicants or therapeutics. Several composite scores have been developed to condense information from multiple toxicity assays for specific compound classes (e.g. endocrine disruptors, halogenated aliphatics), previously[38,39]. Here, we developed NAS using a similar approach to condense the high-dimensional data from MEA recordings into a single measurement with reduced variation that can be used to easily and consistently evaluate compound effects on neural activity, as opposed to analyzing many different parameters individually.

Figure 5. Neural activity score summarizes neural activity for neurotoxicology screening. (**a**–**c**) Examples of NAS calculation for all concentrations of three compounds of varying toxicity from EPA compound libraries analyzed. (**d**–**f**) Concentration–response curves showing how EC_{50} was determined for the same three compounds. Grey dotted line indicates 50% of control NAS AUC, used as a threshold for EC_{50} extrapolation (indicated via red dashed line). Note the lack of extrapolation for aspirin since sufficient effect was not detected. (**g**) Summary of NAS EC_{50} values from Frank et al. 2017[22] and Shafer et al. 2019[21]. (Left) Total compounds with detected effects (EC_{50} within tested range). (Inset) Sensitivity comparisons for NAS vs. average individual MEA parameter and cytotoxicity assays for all compounds with detected effects. Higher sensitivity is defined as lower EC_{50} value.

This reduced variation and improved interpretation could help identify and/or narrow down compounds to examine and develop further, saving time and money wasted on poor candidate compounds. Likewise, improved in vitro studies could help reduce the necessity of in vivo studies, which are expensive, time-consuming, and have ethical and practical concerns due to a myriad of potential endpoint measurements and species differences that can contribute to high variability and difficulty determining true treatment effects[40].

The validation studies presented here indicate that the NAS formula provides an easily interpretable measure of neural network health/functionality and overall effects of perturbation. By compiling all MEA metrics as opposed to individual metrics (i.e., mean firing rate), NAS represents all aspects of neural network function, which can provide more consistent analysis and results interpretation/reporting. Additionally, NAS has the potential to provide increased sensitivity over a collection of individual parameters, as NAS was more sensitive than the individual parameter average for 61.5% of compounds. This result was interesting, demonstrating the utility of implementing relative parameter weights. Since NAS was derived from how all parameters contribute to development/maturation, this result indicates that this approach may describe treatment effects in a more holistic manner than analysis of individual parameters alone, which only describe certain aspects of activity. However, when specific parameters are of interest, we suggest incorporating NAS as an additional metric for screening, not as a complete replacement, as a summary statistic for electrophysiological function and neural network maturation. Additionally, larger training data sets and/or other optimization may allow for improved sensitivity in the future.

Two of the three compounds for which NAS was found to be most sensitive, MPP+ and picoxystrobin, share similar toxic mechanisms, both inhibiting mitochondrial electron transport chain complexes[41,42]. While further research would be needed to determine if this is more than a coincidence, it does suggest mitochondrial function as a sensitive predictor of neurodegeneration. This finding supports a wealth of evidence linking mitochondrial dysfunction to neurodegenerative diseases, in some cases prior to symptom onset and diagnosis[43–45]. Using NAS to analyze and compare various compound classes in more detail may allow for deeper insight into toxicity mechanisms for different compound classes or varying therapeutic potential in drug discovery studies. To this point, the compounds analyzed here were primarily organohalogens, halogenated alkanes, and pyrethroids. Future analysis of additional compound classes with varying properties and mechanisms of actions (e.g., organophosphates) would provide further validation for NAS, as well as additional data on the sensitivity of MEAs and electrophysiological screening to assess developmental neurotoxicity. Indeed, a larger screen of 27 organophosphates detected neurotoxic effects for approximately 1/3rd of tested compounds[21]; however, further studies are needed to make comparisons to the classes examined here and whether other assays may provide higher sensitivity for specific classes of compounds.

Lastly, challenges in analyzing complex and large data sets have been widely acknowledged across multiple assays and techniques, including high-throughput screening, image analysis, and flow cytometry[46–50]. These challenges include high variability, difficulty interpreting results across multiple metrics, and reproducibility—problems that are only exacerbated when examining complex/emergent phenomena that may be difficult to quantify otherwise, such as neuronal network function. While we developed and validated NAS using MEA data, many of the solutions posed for the aforementioned techniques also utilized PCA and other dimensionality reduction methods, suggesting a similar index scoring approach may be useful for these, and other, applications to gain a deeper understanding of important results.

Methods

Cell culture. Mouse HBG3 embryonic stem cell-derived mixed neuronal and glial cells (Aruna Bio, Inc., Athens, GA) were cultured according to previously published protocols[11]. Briefly, cells were thawed and seeded on polyethyleneimine (Sigma Aldrich, St. Louis, MO) and laminin (Sigma)-coated MEA plates (Axion Biosystems, Atlanta, GA) in 6 µL droplets centered over the electrode grids at 40–80,000 cells/well. Cells were maintained with media changes every 3–4 days with full neural culture media consisting of BrainPhys Basal Media (STEMCELL Technologies, Vancouver, BC, Canada) or Advanced DMEM/F12 (ThermoFisher, Waltham, MA) and AB2 Basal Neural Media (ArunA Bio) (1:1) supplemented with 10% (v/v) KnockOut Serum Replacement (ThermoFisher), 2 mM L-glutamine (ThermoFisher), 1% penicillin/streptomycin (ThermoFisher), 0.1 mM β-mercaptoethanol (Sigma), 10 ng/mL glial-derived neurotrophic factor (GDNF) (Peprotech Inc., Rocky Hill, NJ), and 10 ng/mL ciliary neurotrophic factor (CNTF) (Peprotech).

BV2 microglia cells (gift from Dr. Jae-Kyung Lee, University of Georgia, Athens, GA) were cultured according to previously published protocols[51]. Briefly, cells were thawed and seeded on tissue culture-treated plates at approximately 5–10,000 cells/cm^2 and passaged at 60–80% confluency. Cells were maintained with media changes every other day with neural medium consisting of DMEM/F12 (ThermoFisher) supplemented with 5% fetal bovine serum (FBS) (GE Healthcare, Chicago, IL), 2 mM L-glutamine (ThermoFisher), and 1% penicillin/

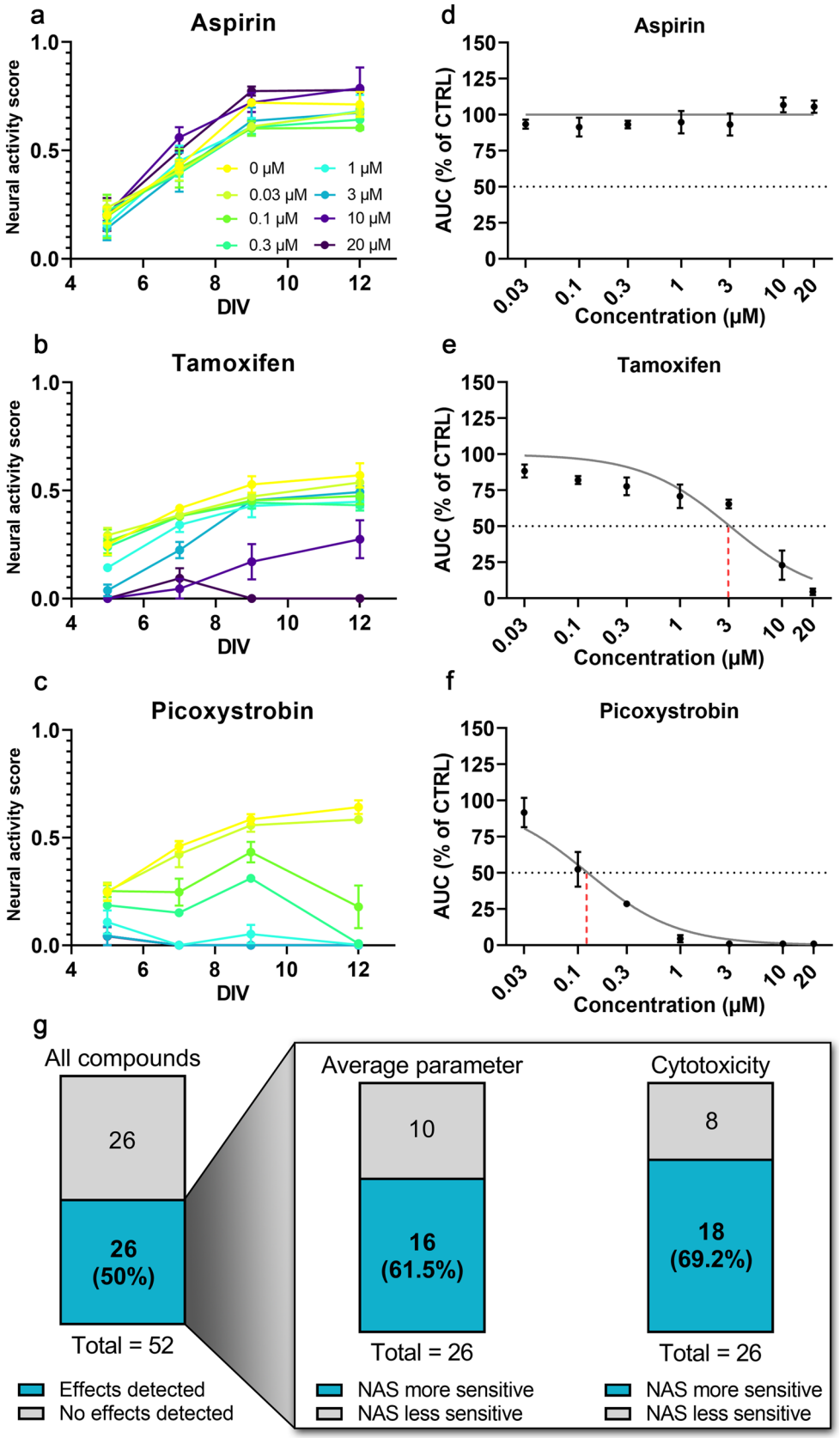
a
Aspirin
Neural activity score
DIV
0 µM
0.03 µM
0.1 µM
0.3 µM
1 µM
3 µM
10 µM
20 µM
b
Tamoxifen
c
Picoxystrobin
d
Aspirin
AUC (% of CTRL)
Concentration (µM)
e
Tamoxifen
f
Picoxystrobin
g
All compounds
26
26 (50%)
Total = 52
Effects detected
No effects detected
Average parameter
10
16 (61.5%)
Total = 26
NAS more sensitive
NAS less sensitive
Cytotoxicity
8
18 (69.2%)
Total = 26
NAS more sensitive
NAS less sensitive

streptomycin (ThermoFisher). For lipopolysaccharide (LPS) treatment, cells were treated with 10 ng/mL or 100 ng/mL LPS in neural medium for 24 h before conditioned media was collected and centrifuged to remove any cells or cellular debris.

MEA preparation, recording, and data processing. 48-well MEA plates (Axion Biosystems) were prepared according to manufacturer's protocol. Briefly, plates were coated with 0.1% polyethyleneimine (PEI) (Sigma) for 1 h at 37 °C, rinsed with sterile water, and allowed to air dry in a biosafety cabinet overnight. The following day, plates were coated with 20 µg/mL laminin (Sigma) for 2 h at 37 °C prior to cell seeding. Mouse neural cultures (see above) were seeded and allowed to adhere for 1 h, then maintained in full neural culture media (see above) supplemented with GDNF (Peprotech) and CNTF (Peprotech) (10 ng/mL each) with media changes every 3–4 days throughout the 3-week recording period.

Neuronal activity was recorded using the Maestro system (Axion Biosystems) and AxIS software v2.1–2.5 (Axion Biosystems) with the following settings: band-pass filter (Butterworth, 300–5000 Hz), spike detector (adaptive threshold crossing, 8xSD of RMS noise), burst detector (100 ms maximum inter-spike interval, 5 spikes minimum, 10 spikes minimum for network bursts, 10 ms mean firing rate detection window). Recordings were performed daily for 2 min at 37 °C after allowing plates to acclimate to the Maestro system.

Raw data files were processed offline using the Statistics Compiler function in AxIS. Statistics Compiler output files were processed in Microsoft Excel (Microsoft Corporation, Redmond, WA) and with custom Python scripts to organize and extract individual parameter data for each well of each MEA plate and for data normalization.

Raster plots generated with Neural Metric Tool v1.2.3 software (Axion Biosystems): https://www.axionbiosystems.com/products/software/neural-module#applications

Neural activity score calculation. After initial data processing, normalization (to z-score values), and outlier removal ($-3 > z > 3$), JMP 14 (SAS Institute, Cary, NC) was used to conduct principal component analysis. All parameters (Supplementary Table S1) were used for all wells (replicates) at 5–19 days in vitro (DIV). The first two principal components were used to visually analyze the temporal separation of the data (Fig. 2a), then the first principal component was used for linear regression analysis to determine the extent of correlation to time. Finally, the factor loadings for the first principal component were calculated to show the extent of contribution for each individual MEA activity parameter (Table 1).

Factor loadings for principal component 1 were then implemented as coefficients in a formula incorporating, and ultimately consolidating, all of the measured individual MEA parameters into an individual index score—NAS—defined as the sum of each measured parameter value multiplied by its factor loading value for each well (replicate) at each time point (Eq. 1).

$$Neural\ activity\ score(NAS) = \sum_{i=1}^{n} \beta_i x_i \tag{1}$$

where β_i are the factor loading values and x_i are the z-normalized measured values for each parameter.

Analysis of DNT hazard screening data. Raw MEA data [*.raw files generated via the Maestro system and AxIS software (Axion Biosystems), see above] from previous studies[21,22] was processed through the same analysis pipeline described above. Additional processing for neurotoxicity data was based on methods described by Shafer et al.[21], including area under curve (AUC) calculation, Hill function fitting, and EC_{50} extrapolation. Specifically, AUC values for each compound and concentration were calculated in Python 3 using the trapezoidal rule (numpy.trapz() function) to integrate normalized NAS values over time (see Data Availability below for more information about custom Python codes). Concentration–response curves (NAS AUC vs. concentration) were generated via nonlinear least squares regression ([Inhibitor] vs. normalized response model) in GraphPad Prism 8.2.0 (GraphPad Software Inc., San Diego, CA) for each compound with Hill slope = − 1.0, and EC_{50} values were extrapolated from the resulting curves.

EC_{50} values corresponding to cytotoxicity (Supplementary Table S2) that were used for sensitivity analysis were reported from previous studies[21,22]. EC_{50} values for NAS and average MEA parameter were calculated as described above.

Statistical analysis. Statistical analysis was performed in GraphPad Prism 8.2.0 (GraphPad Software Inc). Two-way repeated measures analysis of variance (ANOVA) was used to assess differences between treatment groups over time for validation studies unless otherwise noted, and post-hoc tests are stated for individual experiments.

Code and data availability

Custom Python codes and MEA data (.csv files from AxIS Statistics Compiler, compiled into .xlsx file, and analyzed data at several steps) are provided at the following repository: https://doi.org/10.5281/zenodo.3939310.

Received: 25 August 2020; Accepted: 16 February 2021
Published online: 27 April 2021

References

1. Obien, M. E. J., Deligkaris, K., Bullmann, T., Bakkum, D. J. & Frey, U. Revealing neuronal function through microelectrode array recordings. *Front. Neurosci.* **9**, 423 (2015).

2. Johnstone, A. F. M. *et al.* Microelectrode arrays: A physiologically based neurotoxicity testing platform for the 21st century. *Neurotoxicology* **31**, 331–350 (2010).
3. Cotterill, E. *et al.* Characterization of early cortical neural network development in multiwell microelectrode array plates. *J. Biomol. Screen.* **21**, 510–519 (2016).
4. Chiappalone, M. *et al.* Networks of neurons coupled to microelectrode arrays: A neuronal sensory system for pharmacological applications. In *Biosensors and Bioelectronics* vol. 18 627–634 (Elsevier Ltd, 2003).
5. Black, B. J., Atmaramani, R. & Pancrazio, J. J. Spontaneous and evoked activity from murine ventral horn cultures on microelectrode arrays. *Front. Cell. Neurosci.* **11**, 1–10 (2017).
6. Robinette, B. L., Harrill, J. A., Mundy, W. R. & Shafer, T. J. In vitro assessment of developmental neurotoxicity: Use of microelectrode arrays to measure functional changes in neuronal network ontogeny. *Front. Neuroeng.* https://doi.org/10.3389/fneng.2011.00001 (2011).
7. Strickland, J. D., Martin, M. T., Richard, A. M., Houck, K. A. & Shafer, T. J. Screening the ToxCast phase II libraries for alterations in network function using cortical neurons grown on multi-well microelectrode array (mwMEA) plates. *Arch. Toxicol.* **92**, 487–500 (2018).
8. McConnell, E. R., McClain, M. A., Ross, J., LeFew, W. R. & Shafer, T. J. Evaluation of multi-well microelectrode arrays for neurotoxicity screening using a chemical training set. *Neurotoxicology* **33**, 1048–1057 (2012).
9. Illes, S., Fleischer, W., Siebler, M., Hartung, H. P. & Dihné, M. Development and pharmacological modulation of embryonic stem cell-derived neuronal network activity. *Exp. Neurol.* **207**, 171–176 (2007).
10. Wagenaar, D. A., Pine, J. & Potter, S. M. An extremely rich repertoire of bursting patterns during the development of cortical cultures. *BMC Neurosci.* **7**, 1–18 (2006).
11. Wichterle, H., Lieberam, I., Porter, J. A. & Jessell, T. M. Directed differentiation of embryonic stem cells into motor neurons. *Cell* **110**, 385–397 (2002).
12. Latchoumane, C.-F.V. *et al.* Chronic electrical stimulation promotes the excitability and plasticity of ESC-derived neurons following glutamate-induced inhibition in vitro. *Sci. Rep.* **8**, 10957 (2018).
13. Bardy, C. *et al.* Neuronal medium that supports basic synaptic functions and activity of human neurons in vitro. *Proc. Natl. Acad. Sci. U. S. A.* **112**, E2725–E2734 (2015).
14. Aydin, O. *et al.* Development of 3D neuromuscular bioactuators. *APL Bioeng.* **4**, 016107 (2020).
15. Liao, B., Zhao, W., Beers, D. R., Henkel, J. S. & Appel, S. H. Transformation from a neuroprotective to a neurotoxic microglial phenotype in a mouse model of ALS. *Exp. Neurol.* **237**, 147–152 (2012).
16. Chiu, I. M. *et al.* A neurodegeneration-specific gene-expression signature of acutely isolated microglia from an amyotrophic lateral sclerosis mouse model. *Cell Rep.* **4**, 385–401 (2013).
17. Gerber, Y. N., Sabourin, J.-C., Rabano, M., Vivanco, M. D. M. & Perrin, F. E. Early functional deficit and microglial disturbances in a mouse model of amyotrophic lateral sclerosis. *PLoS ONE* **7**, e36000 (2012).
18. Frakes, A. E. *et al.* Microglia induce motor neuron death via the classical NF-κB pathway in amyotrophic lateral sclerosis. *Neuron* **81**, 1009–1023 (2014).
19. Dunlop, J., Bowlby, M., Peri, R., Vasilyev, D. & Arias, R. High-throughput electrophysiology: An emerging paradigm for ion-channel screening and physiology. *Nat. Rev. Drug Discov.* **7**, 358–368 (2008).
20. Shafer, T. J. Application of microelectrode array approaches to neurotoxicity testing and screening. In *Advances in Neurobiology* Vol. 22 275–297 (Springer New York LLC, 2019).
21. Shafer, T. J. *et al.* Evaluation of chemical effects on network formation in cortical neurons grown on microelectrode arrays. *Toxicol. Sci.* **169**, 436–455 (2019).
22. Frank, C. L., Brown, J. P., Wallace, K., Mundy, W. R. & Shafer, T. J. From the cover: Developmental neurotoxicants disrupt activity in cortical networks on microelectrode arrays: Results of screening 86 compounds during neural network formation. *Toxicol. Sci.* **160**, 121–135 (2017).
23. Brown, J. P. *et al.* Evaluation of a microelectrode array-based assay for neural network ontogeny using training set chemicals. *Toxicol. Sci.* **154**, 126–139 (2016).
24. Bal-Price, A. *et al.* Strategies to improve the regulatory assessment of developmental neurotoxicity (DNT) using in vitro methods. *Toxicol. Appl. Pharmacol.* **354**, 7–18 (2018).
25. Nosek, B. A. *et al.* Promoting an open research culture. *Science (80-).* **348**, 1422–1425 (2015).
26. Begley, C. G. & Ellis, L. M. Raise standards for preclinical cancer research. *Nature* **483**, 531–533 (2012).
27. Reality check on reproducibility. *Nature* **533**, 437 (2016).
28. Harrill, J. A., Freudenrich, T. M., Machacek, D. W., Stice, S. L. & Mundy, W. R. Quantitative assessment of neurite outgrowth in human embryonic stem cell-derived hN2^{TM} cells using automated high-content image analysis. *Neurotoxicology* **31**, 277–290 (2010).
29. de Groot, M. W. G. D. M., Westerink, R. H. S. & Dingemans, M. M. L. Don't judge a neuron only by its cover: Neuronal function in in vitro developmental neurotoxicity testing. *Toxicol. Sci.* **132**, 1–7 (2012).
30. Bal-Price, A. K. *et al.* In vitro developmental neurotoxicity (DNT) testing: Relevant models and endpoints. *Neurotoxicology* **31**, 545–554 (2010).
31. Cedarbaum, J. M. *et al.* The ALSFRS-R: A revised ALS functional rating scale that incorporates assessments of respiratory function. *J. Neurol. Sci.* **169**, 13–21 (1999).
32. UPDRS—Parkinson's Disease Research, Education and Clinical Centers. https://www.parkinsons.va.gov/resources/UPDRS.asp. Accessed 10 July 2020.
33. Broderick, J. P., Adeoye, O. & Elm, J. Evolution of the modified Rankin Scale and its use in future stroke trials. *Stroke* **48**, 2007–2012 (2017).
34. Spellicy, S. E. *et al.* Neural stem cell extracellular vesicles disrupt midline shift predictive outcomes in porcine ischemic stroke model. *Transl. Stroke Res.* https://doi.org/10.1007/s12975-019-00753-4 (2019).
35. NINDS Know Stroke Campaign—NIH Stroke Scale. https://www.stroke.nih.gov/resources/scale.htm. Accessed 10 July 2020.
36. Law, C. J., Ashcroft, H. A., Zheng, W. & Sexton, J. Z. Assay development and multivariate scoring for high-content discovery of chemoprotectants of endoplasmic-reticulum-stress-mediated amylin-induced cytotoxicity in pancreatic beta cells. *Assay Drug Dev. Technol.* **12**, 375–384 (2014).
37. Yadav, B. *et al.* Quantitative scoring of differential drug sensitivity for individually optimized anticancer therapies. *Sci. Rep.* **4**, 1–10 (2014).
38. Rotroff, D. M. *et al.* Predictive endocrine testing in the 21st century using in vitro assays of estrogen receptor signaling responses. *Environ. Sci. Technol.* **48**, 8706–8716 (2014).
39. Geiss, K. T., Frazier, J. M. & Dodd, D. E. Toxicity screening of halogenated aliphatics using a novel in vitro volatile chemical exposure system. *NIST Spec. Publ.* **984-4** (2001).
40. Replacing the replacements: Animal model alternatives | Science | AAAS. https://www.sciencemag.org/features/2018/10/replacing-replacements-animal-model-alternatives. Accessed 10 July 2020.
41. Nicklas, W. J., Youngster, S. K., Kindt, M. V. & Heikkila, R. E. IV. MPTP, MPP+ and mitochondrial function. *Life Sci.* **40**, 721–729 (1987).

42. Miguez, M., Reeve, C., Wood, P. M. & Hollomon, D. W. Alternative oxidase reduces the sensitivity of *Mycosphaerella graminicola* to QOI fungicides. *Pest Manag. Sci.* **60**, 3–7 (2004).
43. Lin, M. T. & Beal, M. F. Mitochondrial dysfunction and oxidative stress in neurodegenerative diseases. *Nature* **443**, 787–795 (2006).
44. Johri, A. & Beal, M. F. Mitochondrial dysfunction in neurodegenerative diseases. *J. Pharmacol. Exp. Ther.* **342**, 619–630 (2012).
45. Golpich, M. *et al.* Mitochondrial dysfunction and biogenesis in neurodegenerative diseases: Pathogenesis and treatment. *CNS Neurosci. Ther.* **23**, 5–22 (2017).
46. Kozak, K., Seeliger, J. & Gedrange, T. Multiparametric analysis of high content screening data. *J. Biomed.* **2**, 78–88 (2017).
47. Abraham, Y., Zhang, X. & Parker, C. N. Multiparametric analysis of screening data. *J. Biomol. Screen.* **19**, 628–639 (2014).
48. Caicedo, J. C. *et al.* Data-analysis strategies for image-based cell profiling. *Nat. Methods* **14**, 849–863 (2017).
49. Kvistborg, P. *et al.* Thinking outside the gate: Single-cell assessments in multiple dimensions. *Immunity* **42**, 591–592 (2015).
50. Takahashi, T. Efficient interpretation of multiparametric data using principal component analysis as an example of quality assessment of microalgae. In *Multidimensional Flow Cytometry Techniques for Novel Highly Informative Assays* (InTech, 2018). https://doi.org/10.5772/intechopen.71460.
51. Lee, J.-K., Chung, J., McAlpine, F. E. & Tansey, M. G. Regulator of G-protein signaling-10 negatively regulates NF-κB in microglia and neuroprotects dopaminergic neurons in hemiparkinsonian rats. *J. Neurosci.* **31**, 11879–11888 (2011).

Acknowledgements

The authors would like to thank Dr. Tim Shafer and Dr. Katie Paul-Friedman from the Environmental Protection Agency for sharing data and providing advice on toxicological analysis. The authors would also like to thank Dr. Jae-Kyung Lee at the University of Georgia for providing BV2 cells.

Author contributions

Conceptualization, A.P.P. and S.L.S.; data curation, A.P.P; formal analysis, A.P.P.; funding acquisition, S.L.S.; investigation, A.P.P. and O.A.; methodology, A.P.P., O.A., M.T.A.S., and S.L.S.; project administration, A.P.P. and S.L.S.; resources, A.P.P., O.A., M.T.A.S., and S.L.S.; software, A.P.P.; supervision, M.T.A.S. and S.L.S.; validation, A.P.P. and O.A.; Visualization, A.P.P.; writing—original draft preparation, A.P.P. and S.L.S.; writing—review & editing, A.P.P., O.A., M.T.A.S., and S.L.S.

Funding

Funding was provided by Emergent Behaviors of Integrated Cellular Systems (Grant no. 0939511).

Competing interests

The authors declare no competing interests.

Additional information

Supplementary Information The online version contains supplementary material available at https://doi.org/10.1038/s41598-021-88675-w.

Correspondence and requests for materials should be addressed to S.L.S.

Reprints and permissions information is available at www.nature.com/reprints.

Publisher's note Springer Nature remains neutral with regard to jurisdictional claims in published maps and institutional affiliations.